Smith, W. W., Burnett, R. M., Darling, G. D., & Ludwig, M. L. (1977) *J. Mol. Biol. 117*, 195-225.
Smith, W. W., Pattridge, K. A., & Ludwig, M. L. (1983) *J. Mol. Biol. 165*, 737-755.
Stothers, J. B. (1972) *Carbon-13 NMR Spectroscopy*, pp 313-385 and 2201, Academic Press, New York.
Tauscher, L., Ghisla, S., & Hemmerich, P. (1973) *Helv. Chim. Acta 56*, 630-649.
Van Schagen, C. G., & Müller, F. (1980) *Helv. Chim. Acta 63*, 2187-2201.
Van Schagen, C. G., & Müller, F. (1981) *Eur. J. Biochem. 120*, 33-39.
Vervoort, J., Müller, F., LeGall, J., Bacher, A., & Sedlmaier, H. (1984) in *Flavins and Flavoproteins* (Bray, R. C., Engel, P. C., & Mayhew, S. G., Eds.) pp 269-272, de Gruyter, Berlin.
Vervoort, J., Müller, F., LeGall, J., Bacher, A., & Sedlmaier, H. (1985) *Eur. J. Biochem. 151*, 49-57.
Vinayaka, C. R., & Rao, V. S. R. (1984) *J. Biomol. Struct. Dyn. 2*, 663-674.
Wassink, J. H., & Mayhew, S. G. (1975) *Anal. Biochem. 68*, 609-616.
Watenpaugh, K. D., Sieker, L. C., Jensen, L. H., LeGall, J., & Dubourdieu, H. (1972) *Proc. Natl. Acad. Sci. U.S.A. 69*, 3185-3188.
Watenpaugh, K. D., Sieker, L. C., & Jensen, L. H. (1973) *Proc. Natl. Acad. Sci. U.S.A. 70*, 3857-3860.
Watenpaugh, K. P., Sieker, L. C., & Jensen, L. H. (1975) in *Flavins and Flavoproteins* (Singer, T. P., Ed.) pp 405-410, Elsevier, Amsterdam.
Witanowski, M., Stefaniak, L., & Webb, G. A. (1981) *Annu. Rep. NMR Spectrosc. 11B*, 1-493.

Metabolic Pathways for Ketone Body Production. ^{13}C NMR Spectroscopy of Rat Liver in Vivo Using ^{13}C-Multilabeled Fatty Acids†

Claudia Pahl-Wostl and Joachim Seelig*

Department of Biophysical Chemistry, Biocenter of the University of Basel, CH-4056 Basel, Switzerland

Received April 17, 1986; Revised Manuscript Received July 11, 1986

ABSTRACT: The hormonal regulation of ketogenesis in the liver of living rat has been studied noninvasively with ^{13}C nuclear magnetic resonance. The protocol involved the use of a surface coil that was placed on the skin of the rat, directly over the normal location of the liver. Signals from superficial tissue were suppressed with a 180° pulse at the center of the coil. A resolution of 0.6 ppm was obtained in the ^{13}C NMR spectra at 20.1 MHz, which was equal to or better than that observed in experiments where the liver was surgically exposed and surrounded with radiofrequency coil. The spatial selection for the liver was better than 90%, with extrahepatic adipose tissue contributing only a very small amount of signal. The metabolic activities of the liver were investigated by infusion of ^{13}C-labeled butyrate in the jugular vein of the anesthetized rat. The rate of butyrate infusion was chosen to be close to the maximum oxidative capacity of the rat liver, and the ^{13}C signal intensities were enhanced by using doubly labeled [1,3-^{13}C]butyrate as a substrate. Different ^{13}C NMR spectra and hence different metabolites were observed depending on the hormonal state of the animal. In the *fasted* rat, the most intense ^{13}C signal came from the end product of the Krebs cycle, namely, HCO_3, with additional resonances from glutamine and glutamate. Weak resonances of the ketone bodies 3-hydroxybutyrate and acetoacetate could also be detected and allowed an evaluation of the "redox state" of the in vivo liver. In contrast, 3-hydroxybutyrate was clearly the most important metabolite in the liver of *diabetic* animals, with a weak resonance of HCO_3 as the only other detectable metabolite under in vivo conditions. The ^{13}C NMR studies demonstrate that even when rates of acetyl-CoA production are high, the disposal of this compound is not identical in fasted and diabetic animals. This supports previous suggestions that the redox state of the mitochondrion represents the most important factor in regulation. For a given metabolic state of the animal, different signal intensities were obtained depending on whether butyrate was labeled at C-1, C-3, or C-1,3. From the ratios of incorporation of ^{13}C label into the carbons of 3-hydroxybutyrate, it could be estimated that a large fraction of butyrate evaded β-oxidation to acetyl-CoA but was converted directly to acetoacetyl-CoA. ^{13}C-Labeled glucose could be detected in vivo in the liver of diabetic rats.

A variety of physiological or pathological conditions leads to the enhanced production of acetoacetate and 3-hydroxybutyrate in the body. The two four-carbon organic acids are synthesized by β-oxidation from free acids delivered to the liver, which is the predominant site of ketone body production. The output of ketone bodies depends, however, not only on the rate of fatty acid input but also on the capacity of the liver to generate acetyl-CoA and to dispose of this compound through nonketogenic pathways (McGarry & Foster, 1980). For the same input level of free fatty acids marked differences in the rate of ketone body production have been found de-

† This work was supported by the Kommission zur Förderung der wissenschaftlichen Forschung der Schweiz.

0006-2960/86/0425-6799$01.50/0

pending on whether the animal was fed, fasted, or diabetic.

Metabolic pathways are conveniently studied with radioactively labeled precursors. However, a noninvasive and potentially more versatile approach is the use of ^{13}C nuclear magnetic resonance (^{13}C NMR) in combination with ^{13}C-labeled substrates. The method has recently been adopted for studies of liver biochemistry in living animals (Stevens et al., 1982; Canioni et al., 1983; Alger et al., 1984; Cross et al., 1984; Reo et al., 1984; Siegfried et al., 1985; Stromski et al., 1986). The NMR selection of the liver without the need for abdominal surgery is not trivial and requires special precautions since the liver is a flat and rather curved organ surrounded by adipose tissue with highly mobile triglycerides. The latter give rise to narrow and intense ^{13}C NMR signals, and an admixture of as little as 15% adipose tissue to liver may completely mask the liver resonances proper (Cross et al., 1984). In the present experiments the localization of the liver in the anesthetized rat was achieved with a surface coil. By carefully adjusting the coil position, the shim parameters, and the pulse angle, a liver selection of better than 90% was achieved, confirming our previous results (Cross et al., 1984) and demonstrating the reproducibility of the selection procedure.

In our previous studies [1-^{13}C]butyrate was used as a substrate, and by selecting the carbonyl region of the ^{13}C NMR spectra it was possible to identify the end products of β-oxidation, i.e. the ketone bodies acetoacetate and 3-hydroxybutyrate, as well as oxidation products of the Krebs cycle such as carbonate, glutamine, and glutamate. These earlier investigations have now been extended in several directions. First, we have addressed the question of hormonal control of butyrate oxidation. As a short-chain fatty acid, butyrate does not require the carnitine acyl transferase system to enter the mitochondrial matrix, thus bypassing a major control element of the ketogenesis of long-chain fatty acids. It was therefore of interest to compare the rate of ketone body production in fasted and diabetic rats with labeled butyrate as a substrate. Second, while our first experiments were performed exclusively with [1-^{13}C]butyrate we have now synthesized [3-^{13}C]butyrate as well as doubly labeled [1,3-^{13}C]butyrate. A comparison of the flow of ^{13}C label from the different substrates into the ketone bodies allowed an assessment of the extent to which butyrate was converted to acetoacetate and 3-hydroxybutyrate without prior conversion to acetyl-CoA. In addition, the use of doubly labeled butyrate leads to a distinct improvement in the signal-to-noise ratio. Finally, ketogenesis is usually accompanied by an increased rate of gluconeogenesis. Using [1,3-^{13}C]butyrate as a substrate, we could follow the formation of glucose under in vivo conditions in the liver of diabetic rat.

Materials and Methods

NMR. Fourier transform ^{13}C NMR spectra were obtained in vivo with a Bruker BNT-80 spectrometer with a 1.9-T horizontal magnet having a clear bore of 24 cm. ^{1}H decoupling was performed with a rat-imaging whole-body probe having an inner diameter of 10 cm (Cross et al., 1985). A Waltz eight-pulse sequence was used to obtain complete ^{1}H decoupling with minimal radio frequency power. The liver selection was achieved with a surface coil of 1.8-cm diameter tuned to 20.1 MHz for ^{13}C observation. The experimental conditions were identical with those detailed previously (Cross et al., 1984) with one exception: while in the earlier experiments the anesthetized rat was placed directly onto the surface coil we have now constructed a rat support in which the surface coil remains mobile. With this design it is possible to adjust the position of the surface coil without moving the rat as a whole. The new probe design greatly simplifies the liver selection and also improves the quality of the selection since fine adjustments of the surface coil are easily possible.

Shimming on the rat liver was performed by tuning the ^{13}C surface coil for the ^{1}H frequency of 80 MHz with an impedance transformer (Cross et al., 1984). The best ^{1}H water line width that could be obtained was 25 Hz. ^{13}C NMR spectra were stored at approximately 20-min intervals (1000 acquisitions with a 1.1-s recycle time, a spectral width of 10 kHz, and 2K computer memory).

For the quantitative analysis of the ^{13}C NMR spectra an internal ^{13}C standard is needed. In the present experiments we have chosen the resonance at 54 ppm, which is assigned to the choline methyl groups of phosphatidylcholine. The advantages of this natural-abundance standard are as follows: (1) the resonance is not observed in the adipose tissue surrounding the liver; (2) the resonance is well resolved and does not overlap with the resonances of interest; (3) we have calculated the amplitude ratio of this resonance with the broad carbonyl peak at 175 ppm, which is also characteristic of liver tissue, and found it constant within 5% in all cases evaluated, independent of whether the animal was fed, fasted, or diabetic. All resonance intensities discussed in the following correspond to integrated resonance areas and are normalized with respect to the choline resonance as an internal standard.

A second problem when comparing NMR signal intensities is the possibility of partial saturation due to rapid pulsing. Carbonyl groups are generally characterized by rather long ^{13}C T_1 relaxation times; e.g., for an aequeous solution of butyrate we have measured a relaxation time of $T_1 = 27$ s (at 20.1 MHz), which could require extremely long delay periods in order to record this resonance at its full intensity. The problem is alleviated in liver due to the high content of paramagnetic metal ions in this organ acting as relaxation enhancers. After addition of butyrate to liver homogenates we measured a T_1 relaxation time of $T_1 \approx 3$ s for the carbonyl resonance. In spite of this considerable reduction, the carbonyl resonances are still partially saturated in the in vivo liver spectra shown in this work, mainly for the following reasons. A flip angle of $\alpha = 180°$ (16 μs) was used to minimize superficial tissues adjacent to the surface coil. Even though the flip angle decreases with increasing distance from the surface coil, it can be estimated that inside the liver the flip angle is still $\alpha = 90°$. This together with a recycle delay of 1.1 s lead to a partial saturation of the carbonyl resonance, which can be estimated quantitatively by $M(\tau) = M_0[1 - \exp(-\tau/T_1)]$ (assuming $\alpha = 90°$). With $\tau = 1.1$ s and $T_1 = 3$ s we therefore calculate a saturation factor of $f_s = M(\tau)/M_0 = 0.31$.

The protonated carbon atoms have distinctly shorter T_1 relaxation times. For the C-3 atom of butyrate we determined $T_1 \approx 0.8$ s for liver homogenates. All other experimental conditions unchanged, the saturation factor is then calculated to be $f_s = 0.75$. Under the experimental conditions employed we must hence take into account the differential saturation of protonated and nonprotonated ^{13}C resonances. Assuming equal concentrations of ^{13}C label at carbon atoms $^{13}C(1)$ and $^{13}C(3)$ of butyrate, we expect an integrated intensity ratio of $^{13}C(3)/^{13}C(1) = 0.75/0.31 = 2.4$; i.e., the integrated intensity of the carbonyl $^{13}C(1)$ resonance in the in vivo liver spectra is smaller than that of the $^{13}C(3)$ resonance by a factor 2.4. It could be argued that the above saturation formula is too crude an approximation for the inhomogeneous B_1 field of a surface coil. [1,3-^{13}C]Butyrate was therefore injected into excised liver and the liver measured with the surface coil under the same experimental conditions as in the in vivo experiments. In addition, the same sample was measured under fully relaxed

conditions. A comparison of the two experiments yielded a saturation factor of C(3)/C(1) = 2.0, in good agreement with the theoretical estimate.

The in vitro spectroscopy was performed on a Bruker CXP-300 NMR spectrometer operating at 75.5 MHz for ^{13}C. A 10-mm carbon probe was used for spectra of excised tissue and tissue extracts. Broad-band proton decoupling was applied only during the acquisition time to avoid NOE effects. Pulse angle and relaxation delay were chosen to yield fully relaxed ^{13}C signal intensities, avoiding the necessity of correction factors. Chemical shift referencing was accomplished with a Me_4Si capillary.

Chemicals. [1-^{13}C]Butyrate (90% enrichment) was synthesized according to the procedure of Heussler et al. (1975). [1,3-^{13}C]Butyrate (90% enrichment) was prepared from CH_3I by three chain elongations with CO_2. In the first and third elongation step $^{13}CO_2$ was employed. The overall yield in the eight-step synthesis was 5%, based on the amount of $Ba^{13}CO_3$ employed in the first Grignard reaction.

Animals. Male rats (Sprague–Dawley strain, 250–300 g) were used for all experiments. They were fed ad libitum with standard rat chow. Fasted rats were deprived of food for 24 h prior to use. Experimental diabetes was induced by the intraveneous injection of streptozotocin (90 mg/kg body weight). Animals were used 48 h later if they proved to be acutely ketotic as determined by an immediate strongly positive urine test for ketones (Keto merckognost; Merck, Darmstadt). Diabetic rats were fed ad libitum.

Infusion Experiments. Rats were anesthetized with pentobarbital (50 mg/kg, intraperitoneally). A catheter was placed in the right jugular vein and maintained patent with isotonic saline solution infused at 0.5 mL/h. The labeled butyrate was infused as a 0.2 M solution (pH 7.3). The infusion rate was adjusted to 6 mL/h corresponding to 80–100 μmol/min per kg body weight. In order to obtain maximal rates of ketogenesis the infusion rate was first calculated according to data from experiments with ^{14}C-labeled substrates (McGarry & Foster, 1971; Bates et al., 1968) and was finally adjusted to be close to maximum metabolic capacity of liver in fasted animals.

For the extracts and for the in vitro spectra the liver was excised after termination of the infusion and immediately frozen in liquid nitrogen. For high-resolution spectra at 300 MHz the liver was sliced and transferred into a 10-mm NMR sample tube. The temperature was kept at 37 °C.

Results

Figure 1 displays in vivo ^{13}C NMR spectra of the liver of a fasted rat. [1,3-^{13}C]butyrate was infused into the liver via the jugular vein over a period of about 100 min. The optimal conditions for liver selection were determined by minimizing the triglyceride carbonyl resonance at 171 ppm, which appears as a sharp peak superimposed on the broader carbonyl resonances of the liver [cf. Cross et al. (1984)]. From the intensity of this peak one can estimate that the liver selection was better than 90%, with extrahepatic fatty tissue contributing less than 10%. Figure 1A represents the state of the liver at the beginning of infusion, Figure 1B represents the situation after an infusion period of about 100 min, and Figure 1C is the difference spectrum (B – A). The assignment of the resonances is detailed in the figure legend and in Table I. In the difference spectrum 1C, the natural-abundance ^{13}C background is essentially eliminated and only resonances from metabolized [1,3-^{13}C]butyrate are retained. Most resonances in Figure 1C are clustered in the carbonyl region (160–190 ppm) of the ^{13}C NMR spectrum and can be assigned to the

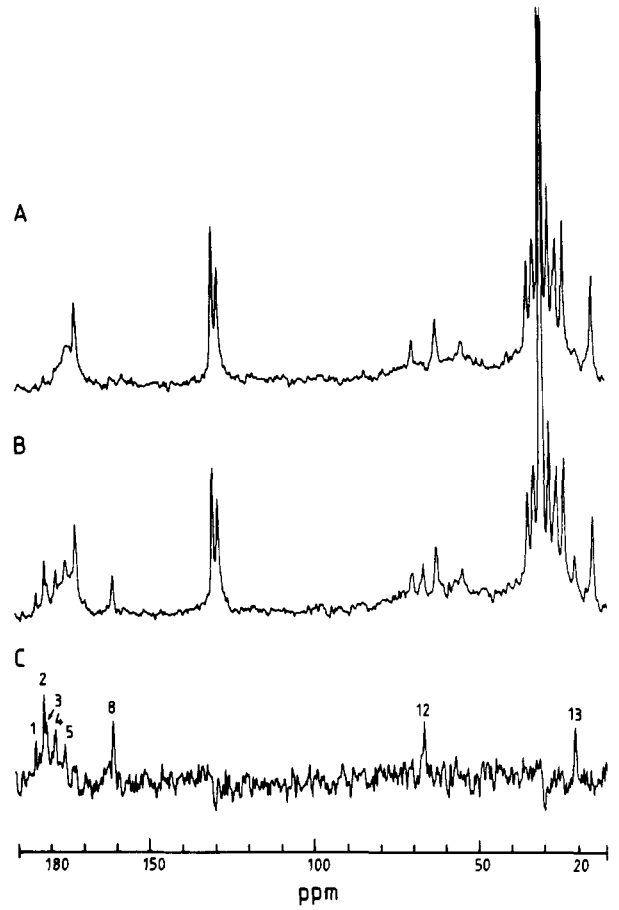

FIGURE 1: ^{13}C NMR spectra of in vivo rat liver observed in a *fasted* animal. Spectra obtained at 20.1 MHz with a surface coil and a ^{13}C 180° surface nulling pulse. Proton decoupling employed only during the 100-ms acquisition time. [1,3-^{13}C]Butyrate infused via the jugular vein over a period of 110 min. (A) Spectral acquisition from 20 min before to 20 min after start of infusion. (B) Spectral acquisition for the period 80–120 min after start of infusion. (C) Difference spectrum (B – A) showing only resonances of metabolized [1,3-^{13}C]butyrate. Assignment of the resonances according to Table 1. Each spectrum represents 2000 acquisitions. Artifical line broadening of 4 Hz.

Table I: Assignment of ^{13}C Resonances

resonance	chemical shift (ppm)	assignment
1	184.0	C-1 butyrate
2	181.4	C-5 glutamate
3	180.5	C-1 β-hydroxybutyrate
4	177.8	C-5 glutamine
5	175.0	C-1 acetoacetate
6	174.7	C-1 glutamate
7	174.2	C-1 glutamine
8	160	carbonate
9	76.1	C-3 β-glucose
10	73.2	C-3 α-glucose
11	70.1	C-4 α,β-glucose
12	65.7	C-3 β-hydroxybutyrate
13	19.4	C-3 butyrate

C(1) atoms of butyrate, acetoacetate, and 3-hydroxybutyrate as well as to the C(5) atoms of glutamine and glutamate. Clearly visible is the carbonate resonance at 160 ppm. In addition to the carbonyl resonances, the C(3)-methylene resonance of butyric acid (19.4 ppm) and the C(3) resonance of 3-hydroxybutyrate (65.7 ppm) can also be detected.

In Figure 2 the [1,3-^{13}C]butyrate infusion experiment was repeated with a diabetic rat. The difference spectrum 2C shows a simpler pattern compared to that of fasted rat (Figure 1C). Well resolved are the resonances of the substrate (butyrate) and again carbonate. Resonances of the amino acids

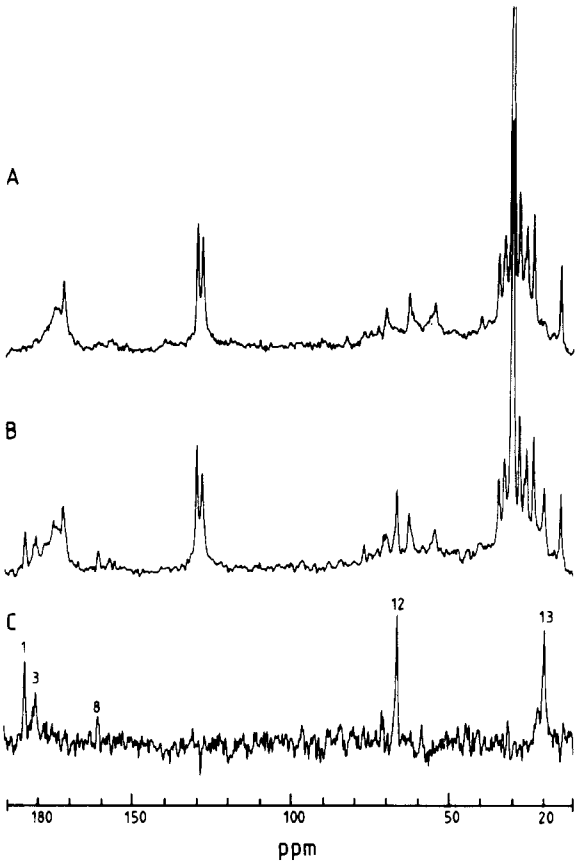

FIGURE 2: ^{13}C NMR spectra of in vivo rat liver observed in a *diabetic* animal. Infusion of [1,3-^{13}C]butyrate. Other experimental conditions as in Figure 1. (A) Spectral acquisition from 20 min before to 20 min after start of infusion. (B) Spectral acquisition 80–120 min after start of infusion. (C) Difference spectrum (B – A) showing intrahepatic metabolites derived from [1,3-^{13}C]butyric acid (cf. Table 1 for assignment).

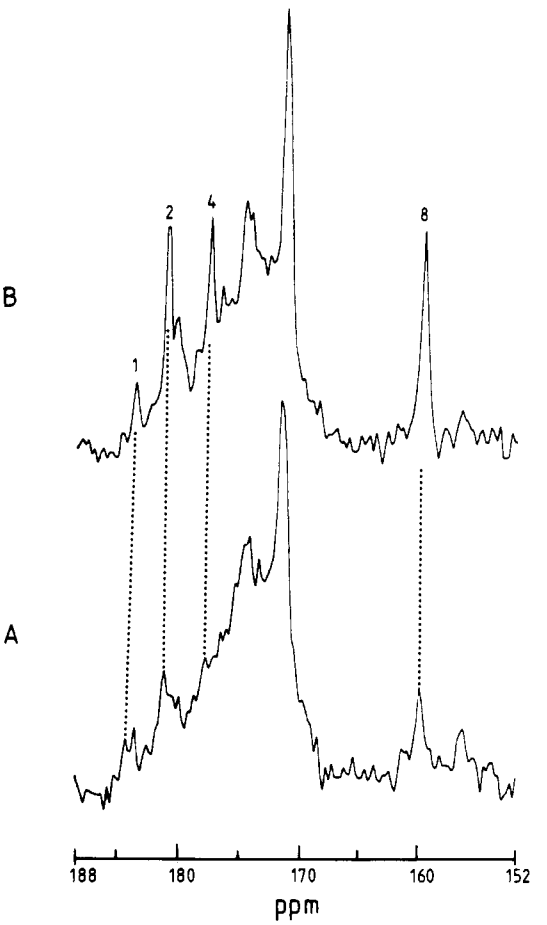

FIGURE 3: ^{13}C NMR spectra of in vivo rat liver of a *fasted* animal. Infusion of (A) [1-^{13}C]butyrate and (B) [1,3-^{13}C]butyrate over a period of 110 min. Only the carbonyl region shown. Spectra acquired in the period 20–140 min after start of infusion (6000 scans). All other conditions as in Figure 1. Same number of resonances in both spectra, but with distinctly increased intensities for [1,3-^{13}C]butyrate: resonance 1, butyrate; resonance 2, 4, and 8, metabolites of the Krebs cycle (cf. Table 1 for assignment).

and of acetoacetate are missing; instead the C(1) and C(3) resonances of 3-hydroxybutyrate are distinctly enhanced compared to those in fasted rat.

Figures 1 and 2 provide direct evidence for the metabolic activity of liver in vivo and its ketogenic response to butyrate infusion. The production of ketone bodies is observed in both the fasted and the pathological state but is distinctly enhanced in diabetic rat. On the other hand, metabolites of the Krebs cycle are mainly observed in the fasted rat. The intensity of the carbonate peak in diabetic rat is much reduced compared to that of fasted rat.

The advantages of using doubly labeled [1,3-^{13}C]butyrate vs. monolabeled [1-^{13}C]butyrate are demonstrated in Figures 3 and 4. Figure 3 shows the carbonyl resonances (150–190 ppm) of in vivo liver spectra of fasted rat after infusion of [1-^{13}C]butyrate (3A) and [1,3-^{13}C]butyrate (3B). Both spectra reveal essentially the same number of metabolite resonances, but the individual signals are clearly more discernible in the case of [1,3-^{13}C]butyrate. While some of the intensity increase was due to the improved B_0 homogeneity, the more important factor was the increase in ^{13}C label concentration. According to the classical scheme of β-oxidation, [1,3-^{13}C]butyrate should be split in the liver into two molecules of [1-^{13}C]acetyl-CoA, thus doubling the concentration of ^{13}C label in the acetyl-CoA pool compared to monolabeled [1-^{13}C]butyrate.

A similar comparison is shown in Figure 4 for the diabetic rat. Under these conditions the most conspicuous differences were noted in the region of the hydroxylated carbon atoms (50–80 ppm), where the C(3) resonance of 3-hydroxybutyrate (65.7 ppm) was found to be much increased after infusion of [1,3-^{13}C]butyrate (4B) compared to the infusion of the monolabeled substrate (4A). In addition, Figure 4B shows new resonances at 70.1 and 76.1 ppm that can be assigned to glucose as discussed below.

If it is assumed that all butyrate is split into two molecules of acetyl-CoA, infusion of [1-^{13}C]butyrate and [3-^{13}C]butyrate should produce the same intermediate, namely [1-^{13}C]-acetyl-CoA. If it is further assumed that ^{13}C-labeled acetyl-CoA and acetyl-CoA produced from endogenous substrate enter a common pool, disposal of this compound through ketogenic and nonketogenic pathways should then result in the same ^{13}C-labeling pattern and hence identical ^{13}C NMR spectra regardless of whether the starting compound was labeled at the C-1 or the C-3 position. This was, however, not borne out experimentally as is illustrated in Figure 5. Diabetic rats were infused with [1-^{13}C]butyrate, [3-^{13}C]butyrate, or [1,3-^{13}C]butyrate. At about 30 min after the end of the infusion, the animals were sacrificed and ^{13}C NMR spectra were recorded of the excised liver (at 75 MHz). Focussing the discussion on the C(1) (180.5 ppm) and C(3) (65.7 ppm) resonances of the ketogenic end product 3-hydroxybutyrate, it is obvious that infusion of [3-^{13}C]butyrate enhanced the C(3) resonance of 3-hydroxybutyrate (Figure 5A) while infusion of [1-^{13}C]butyrate lead to a preferential labeling of the C(1)

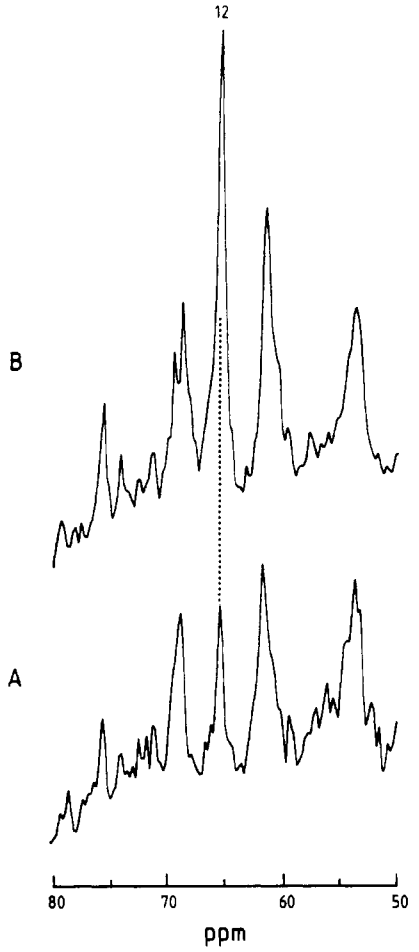

FIGURE 4: ^{13}C NMR spectra of in vivo rat liver of a *diabetic* animal. Infusion of (A) [1-^{13}C]butyrate and (B) [1,3-^{13}C]butyrate over a period of 110 min. Only the region of the hydroxylated carbon atoms shown. Resonance 12 absent prior to infusion and can be assigned to C-3 of 3-hydroxybutyrate. An almost fourfold increase in intensity of this resonance is observed when [1,3-^{13}C]butyrate is infused instead of the monolabeled substrate.

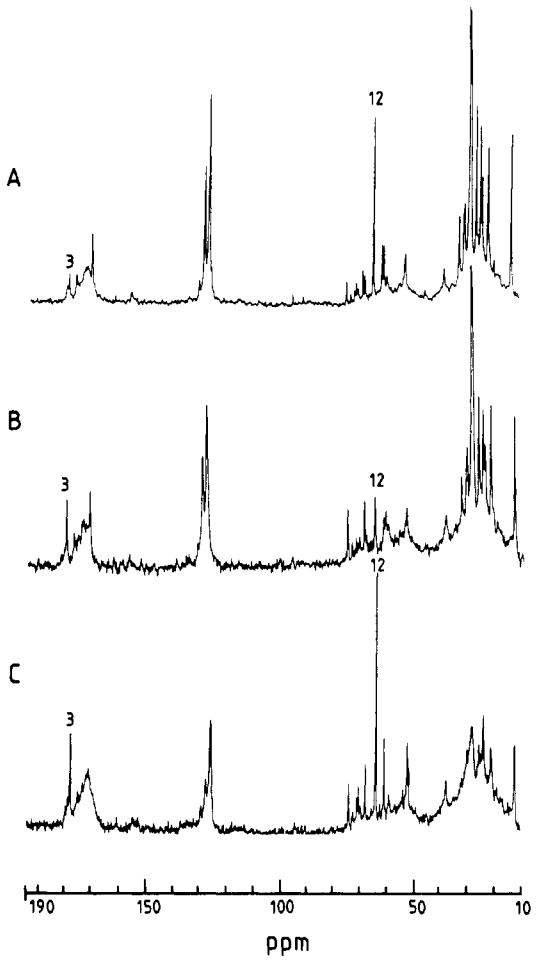

FIGURE 5: Comparison of ^{13}C NMR spectra of three diabetic rat liver preparations after infusion of (A) [3-^{13}C]butyrate, (B) [1-^{13}C]butyrate, and (C) [1,3-^{13}C]butyrate. The livers excised 30 min after end of infusion and measured at 75.5 MHz. Resonances 3 and 12 assigned to C(1) and C(3), respectively, of 3-hydroxybutyrate. NMR parameters were chosen to ensure fully relaxed spectra; the resonance intensities are therefore comparable without applying saturation factors. Infusion of [3-^{13}C]butyrate leads to an enhancement of the C-3 resonances of 3-hydroxybutyrate, and that of [1-^{13}C]butyrate, to an enhancement of the C-1 resonance. Measuring temperature, 37 °C.

carbon (Figure 5B). The infusion of [1,3-^{13}C]butyrate served as a control and indicated an enhanced ^{13}C labeling at both carbon atoms. These experiments provide evidence against a complete scrambling of the ^{13}C label via a common intermediate [1-^{13}C]acetyl-CoA; instead they suggest that at least part of the substrate is converted directly into 3-hydroxybutyrate, bypassing the general acetyl-CoA pool.

The formation of ketone bodies is normally accompanied by an enhanced rate of gluconeogenesis (Cahill, 1981). With [1,3-^{13}C]butyrate as a substrate it was possible to follow the flow of ^{13}C label into glucose under in vivo conditions. Figure 6 shows a series of in vivo liver spectra of a diabetic rat during and after infusions of the substrate. Only the 50–80 ppm region, characteristic of hydroxylated carbon atoms, is displayed. At the beginning of the experiment the spectrum consists of essentially three natural-abundance ^{13}C resonances that are assigned to the methyl groups (54 ppm) of the phosphocholine head group of the phospholipids and the C(2) (62.2 ppm) and C(1,3) (69.2 ppm) resonances of the glycerol backbone of triglycerides. During the course of infusion two new resonances at 70.1 and 76.1 ppm are detected (in addition to the strong signal of 3-hydroxybutyrate discussed above), which arise from the incorporation of ^{13}C label into the carbon atoms C(4) and C(3) of glucose, respectively. We have also investigated gluconeogenesis in fasted rats and also with monolabeled butyrate as a substrate. It was generally difficult to detect glucose formation under in vivo conditions since the signal intensities were rather weak. However, with excised liver or with perchloric acid extracts of excised liver the formation of ^{13}C-labeled glucose was easily verified even under the conditions defined above.

Table II: Distribution of ^{13}C in 3-Hydroxybutyrate Measured in Perchloric Acid Extracts of the Liver of Fasted and Diabetic Rats[a]

animal	substrate	C-1/C-3 ratio[b]	no. of expts
fasted rat	[1-^{13}C]butyrate	2.0 ± 0.1	2
	[3-^{13}C]butyrate	0.4 ± 0.005	2
	[1,3-^{13}C]butyrate	0.9 ± 0.1	2
diabetic rat	[1-^{13}C]butyrate	2.3 ± 0.7	3
	[3-^{13}C]butyrate	0.3 ± 0.05	2
	[1,3-^{13}C]butyrate	0.7	1

[a] The animal was sacrificed at the peak of 3-hydroxybutyrate production. [b] The intensity ratios are corrected for partial saturation by comparison with a solution of pure 3-hydroxybutyrate.

For each type of labeled butyric acid at least two independent in vivo experiments were performed (cf. also Table II). The integrated signal intensities were referred to the natural-abundance choline resonance. Under these conditions the reproducibility of the data was extremely good. The average variation after evaluating 4 different resonances (C(5)

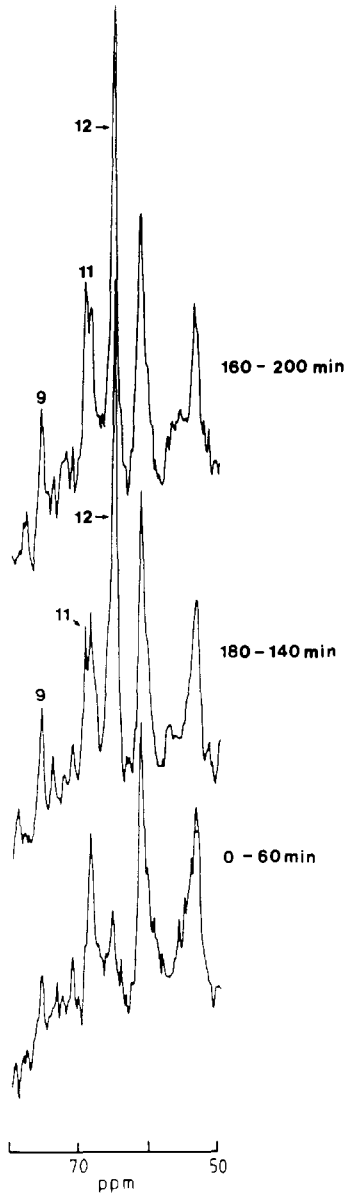

FIGURE 6: Gluconeogenesis in *diabetic* rat. ^{13}C NMR spectra of in vivo rat liver after infusion of [1,3-^{13}C]butyrate showing the appearance of three additional resonances in the region of hydroxylated carbon atoms (50–80 ppm). Besides 3-hydroxybutyrate (resonance 12) [3-^{13}C]-β-glucose and [4-^{13}C]-α,β-glucose (resonances 9 and 11, respectively) are observed. Assignment confirmed by measurement of perchloric acid extracts. NMR parameters as in Figure 1.

Glu, C(1) Hybu, C(3) Hybu, CO_2) in a total of 11 in vivo experiments was ±9 % (maximum ±19 %, minimum ±1 %).

Discussion

Sensitivity of ^{13}C NMR for in Vivo Liver Studies. As a prerequisite for the biochemical analysis let us briefly consider the sensitivity of the ^{13}C NMR method. A spectral resolution of 0.6 ppm (full width at half-height) was achieved under in vivo conditions at 20.1 MHz, and the sensitivity was sufficient to detect metabolites at concentrations as low as 0.5–1 mM. Considerably lower concentrations could be measured in in vitro experiments at 75.5 MHz due to the higher B_0 field and the more favorable coil design. The sensitivity of ^{13}C NMR may be illustrated with the resonances of [1,3-^{13}C]butyrate as shown in Figures 1 and 2. This substrate was delivered to the liver at a constant concentration of about 2 mM in the blood plasma. In the liver, [1,3-^{13}C]butyrate was converted rapidly into other metabolites. Nevertheless, the characteristic resonances of the [1-^{13}C]carbonyl group (at 184 ppm) and the [3-^{13}C]CH_2 group (at 19.4 ppm) were still observable in the fasted as well as in the diabetic rat. In the fasted liver, the butyrate resonances were rather weak and a butyrate concentration of 1–2 mM was estimated by comparison with external standards and by measurement of excised liver. In contrast, a distinctly higher butyrate concentration of ca. 4–5 mM was observed in the diabetic rat (cf. Figures 1C and 2C). The observation of butyrate in fasted and diabetic rat demonstrates that the livers were working close to maximal capacity in both physiological states. The different butyrate intensities in the ^{13}C NMR spectra may then be explained not so much by different enzymic capacities of fasted and diabetic liver as by the availability of long-chain free fatty acids as competing substrates for oxidation. In the fasted rat the blood concentration of long-chain free fatty acids was estimated to be about 0.8 mM but increased to about 2 mM in diabetic rat (Blackshear & Alberti, 1974). Thus, the oxidation rate of [1,3-^{13}C]butyrate in diabetic liver was reduced because of the abundance of competing long-chain free fatty acids, leading to a transitory accumulation of the substrate.

Regulation of Butyrate Oxidation in in Vivo Liver. The production of ketone bodies in the liver is controlled at at least three different levels [cf. Mayes and Laker (1981)]: (1) regulation of the supply of free fatty acids from peripheral fat depots to the liver; (2) intrahepatic regulation of the channeling of long-chain acyl-CoA into the pathways of esterification and β-oxidation; (3) regulation of the production of acetyl-CoA in the mitochondrion and of the disposal of this compound either via the Krebs cycle or via the formation of ketone bodies.

In the present experiments regulation at the first two levels can be excluded for the following reasons: First, ^{13}C-labeled butyrate was supplied to the liver at an approximately constant concentration in the blood plasma of about 2 mM, and only the concentration of long-chain free fatty acids varied with the physiological state of the animal. Second, as a short-chain fatty acid butyrate is known not to be utilized directly in the esterification and the formation of triglycerides. Third, butyrate enters the mitochondrion by a transport mechanism that is independent of the carnitine acyl transferase system (Aas & Brenner, 1968). Hence, it is not the rate of butyrate delivery to the liver but the generation of ^{13}C-labeled acetyl-CoA, its competition with nonlabeled acetyl-CoA (produced from endogenous long-chain free fatty acids) as well as the partitioning of this compound between the pathways of oxidation to CO_2, and conversion into ketone bodies that is of major importance in the present context.

The production of acetyl-CoA was not directly observable in the ^{13}C NMR spectra. However, following the time course of the various metabolites and comparing of their intensities provided indirect insight into the generation ^{13}C-labeled acetyl-CoA. Figure 7 summarizes the time courses of the most important ^{13}C-labeled metabolites. Each time course was normalized with respect to the maximum intensity of the corresponding ^{13}C resonance. The end of the butyrate infusion (which lasted for about 100–110 min) is indicated by an arrow. As mentioned above, ^{13}C-labeled metabolites with concentrations of less than 0.5 mM were below the sensitivity limit of the NMR method under in vivo conditions. On an absolute scale the data points of Figure 7 thus encompass a concentration range of 0.5–5 mM. Figure 7A represents the time course of [1,3-^{13}C]butyrate in diabetic liver in vivo. The figure clearly demonstrates that the substrate accumulates in the diabetic liver, which was explained above by the high concentration of competing long-chain free fatty acids. The

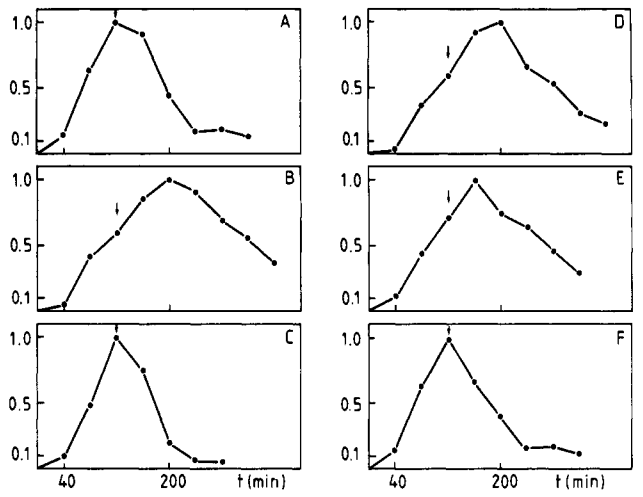

FIGURE 7: Time course of metabolites derived from [1,3-^{13}C]butyrate observed in the liver of living rat. Intensity of each resonance normalized with respect to its maximum: (A) diabetic rat, C(3) of butyrate (at 19.4 ppm); (B) diabetic rat, C(3) of 3-hydroxybutyrate (65.7 ppm); (C) fasted rat, C(3) of 3-hydroxybutyrate (65.7 ppm); (D) fasted rat, HCO_3 (160 ppm); (E) fasted rat, C(5) of glutamine (177.8 ppm); (F) fasted rat, C(5) of glutamate (181.4 ppm). End of the infusion marked by an arrow.

production of 3-hydroxybutyrate in fasted rat (Figure 7C) followed the same time course as butyrate accumulation but lagged behind in the liver of diabetic animal (7B). The remaining graphs describe concentration changes in the fasted animal and refer to carbonate (7D), glutamine (7E), and glutamate (7F). Maximum intensity was observed for glutamate at the end of the butyrate infusion, whereas the concentration maxima of glutamine and carbonate lagged behind by 20 and 40 min, respectively. The shift in the concentration maxima correlates with the sequence of events in the Krebs cycle where glutamine is generated from glutamate, while CO_2 is the final product of the oxidation process. The close similarity in the time course of the major metabolites 3-hydroxybutyrate in diabetic rat (7B) and carbonate in fasted rat (7D) together with the approximate agreement in absolute concentration of these end products of ketogenesis and Krebs cycle activity, respectively, suggests that the oxidative capacities of in vivo liver were rather similar for fasted and diabetic rat.

Metabolic Differences between Diabetic and Fasted Rat Liver. In spite of similar oxidation rates the metabolic events following butyrate infusion were quite different for fasted and diabetic animals under in vivo conditions. The comparison of the ^{13}C NMR spectra of in vivo liver of fasted rat (Figure 1C) and diabetic rat (Figure 2C) reveals different metabolic patterns for the two physiological states, with carbonate and glutamate as the major metabolites in the fasted animal and 3-hydroxybutyrate as the most important metabolite in the diabetic liver. Thus, depending on the physiological state of the animal, acetyl-CoA was predominantly channeled into either the Krebs cycle (fasted rat) or the ketogenic pathway (diabetic rat).

In the fasted animal additional resonances were observed for [5-^{13}C]glutamine, [1-^{13}C]-3-hydroxybutyrate, and [1-^{13}C]acetoacetate, providing in vivo confirmation for well-established biochemical pathways. [5-^{13}C]Glutamate and [5-^{13}C]glutamine were produced from [5-^{13}C]-α-ketoglutarate which, in turn, was generated in the Krebs cycle starting with the addition of [1-^{13}C]acetyl-CoA to oxaloacetate. However, none of the at least five intermediates between [1-^{13}C]-acetyl-CoA and [5-^{13}C]glutamate rose to large enough concentrations to be detectable in the in vivo liver. On the other hand, perchloric acid extracts of the fasted liver showed weak additional resonances for [1-^{13}C]glutamate and [1-^{13}C]glutamine (cf. Figure 8A). This result can be explained if part of the [5-^{13}C]-α-ketoglutarate remained in the Krebs cycle, generating [1-^{13}C]oxaloacetate that was then used in a second turn of the cycle.

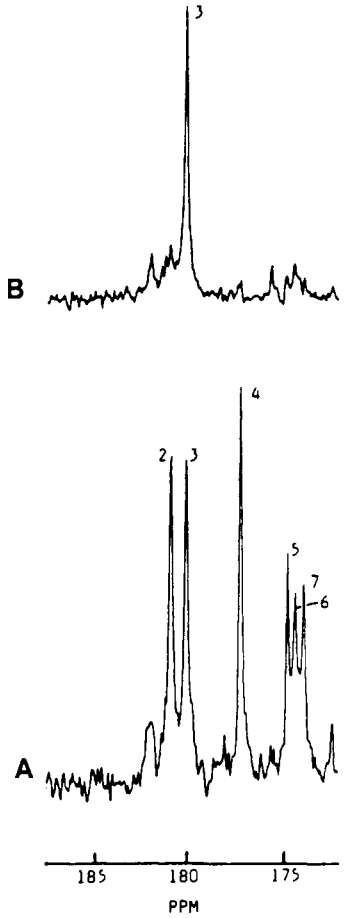

FIGURE 8: ^{13}C NMR spectra (at 75.5 MHz) of the perchloric acid extracts of rat liver after infusion of [1,3-^{13}C]butyrate. The liver excised 10 min after the end of infusion. The carbonyl region shown for (A) a fasted animal and (B) a diabetic animal. The latter spectrum is dominated by 3-hydroxybutyrate (resonance 3); resonances of the Krebs cycle (resonances 2, 4, 6, and 7) as well as those of ketone bodies (resonances 3 and 5) are shown for the fasted animal. It may be noted that resonances 5–7 cannot be resolved under in vivo conditions (cf. the corresponding in vivo spectrum Figure 1C). NMR parameters: 5000 acquisitions; 6-s relaxation delay; 40° flip angle (8 μs); 4-Hz line broadening. Assignment of resonances as in Table I.

The simultaneous observation of 3-hydroxybutyrate and acetoacetate allowed an approximate evaluation of the "redox state" of the liver. The latter may be defined as the concentration ratio [3-hydroxybutyrate]/[acetoacetate] where a shift toward 3-hydroxybutyrate is equivalent to a more reduced redox state [cf. Berry et al. (1983), and Owen and Schramm (1981)]. From the amplitudes of the corresponding carbonyl resonances (Figure 1C) a [3-hydroxybutyrate]/[acetoacetate] ratio of 1.4 was evaluated. However, this value must be considered as a lower limit since the acetoacetate resonance (resonance 5; 175 ppm) may also contain contributions from glutamate (174.7 ppm) and glutamine (174.2 ppm). This is illustrated by the 75.5-MHz spectrum of the perchloric acid extract of liver from fasted rat (Figure 8A) where all three resonances are clearly resolved.

The [3-hydroxybutyrate]/[acetoacetate] ratio as determined from the amplitudes of resonances 3 and 5 of Figure 8 was

1.6. The in vivo results were found to be in broad agreement with in vitro studies. For hepatocytes derived from starved rats, [3-hydroxybutyrate]/[acetoacetate] ratios between 0.2 and 3.0 have been reported, depending on the chain length and concentration of the exogeneous fatty acid supplied, on the incubation time, and on a variety of other conditions (Siess et al., 1982; Berry et al., 1983).

Only 3-hydroxybutyrate but not acetoacetate could be detected in diabetic liver under in vivo conditions, which meant that the acetoacetate concentration was definitely below 1 mM. However, acetoacetate could be observed in the perchloric acid extract of liver of diabetic rat (Figure 8B) from which a [3-hydroxybutyrate]/[acetoacetate] ratio of about 10 was estimated. Taken together, the in vivo and in vitro measurements provide evidence for a more reduced redox state of the diabetic liver as compared to fasted liver. These results lend support to the previously held view that the redox state of the liver is of primary importance in regulatory terms (Wieland, 1968; Siess et al., 1982). A more reduced redox state of the liver is equivalent to an increased concentration of NADH. This, in turn, induces an increase in 3-hydroxybutyrate and a simultaneous decrease of free oxaloacetate (assuming that malate dehydrogenase and 3-hydroxybutyrate dehydrogenase are at equilibrium and share the same NAD^+ pool). The differences in ketogenesis between fasted and diabetic rat would thus be explained by the control of acetyl-CoA disposal via the redox potential of the liver.

The present results are at variance with in vitro studies on perfused liver in which radioactive [1-^{14}C]octanoate was used as a substrate (McGarry & Foster, 1971). Octanoate, just as butyrate, enters the mitochondrion independently of the carnitine shuttle and is also not used in triglyceride synthesis. At high levels of octanoate the livers from fasted animals were found to manufacture ketone bodies at rates comparable to those of livers from diabetic rat. In addition, the activity of the Krebs cycle appeared to be only modestly depressed in the diabetic group. It was concluded that the rapid rates of ketogenesis observed in perfused livers from both fasted and diabetic animals resulted primarily from an overproduction of acetyl-CoA as opposed to a diminished oxidation of this substrate through the Krebs cycle. In contrast, the ^{13}C NMR studies on in vivo liver demonstrate an enhanced production of 3-hydroxybutyrate and a suppression of Krebs cycle activity in the diabetic animal. In order to eliminate a unique effect of butyrate, additional ^{13}C NMR experiments were performed with [1,3-^{13}C]octanoate (Pahl, C. & Sellig, J., unpublished work). The results were virtually identical with those obtained for butyrate. Under in vivo conditions the major metabolites in the liver of the fasted animal were those of the Krebs cycle, while 3-hydroxybutyrate was the predominant metabolite in the diabetic animal. Again the rate of ketone body production was quite different in the two hormonal states and thus at variance with the perfused liver studies.

Pathways of 3-Hydroxybutyrate Formation. In the liver, 3-hydroxybutyrate is produced exclusively by reduction of acetoacetate with NADH. When the incorporation of ^{13}C label is traced from butyrate into 3-hydroxybutyrate, the discussion can thus be confined to the formation of its precursor acetoacetate. Two different pathways need to be considered. In the first, butyrate would undergo β-oxidation and two molecules of acetyl-CoA would be fed into a common pool of acetyl-CoA, with both [1-^{13}C]butyrate and [3-^{13}C]-butyrate yielding [1-^{13}C]acetyl-CoA. Acetoacetate would then be formed by condensation of acetyl-CoA via the rather complex (hydroxymethyl)glutaryl pathway [cf. Lynen et al. (1958) and McGarry and Foster (1980)]. As a net result, ^{13}C label should appear with equal intensity at C-1 and C-3 of 3-hydroxybutyrate. In the second pathway, the butyrate molecule would first be transformed into acetoacetyl-CoA. At this stage of the oxidation process the carbon skeleton would still retain the original labeling pattern. However, acetyl-CoA from the common pool would be added next, and the resulting hydroxymethylglutaryl-CoA would be split into acetoacetate and acetyl-CoA. In this mechanism, carbon atoms 1 and 2 of butyrate would be exchanged against acetyl-CoA of the common pool whereas carbon atoms 3 and 4 would not be replaced and would appear at identical positions in acetoacetate and 3-hydroxybutyrate. Thus, a comparison of the C-1/C-3 ratios for different substrate should shed light on the activity of the two pathways. Table II summarizes the C(1)/C(3) ratios as observed with ^{13}C NMR in the rat liver of fasted and diabetic animals. Inspection of Table II allows the following conclusions. First, both pathways are activated under in vivo conditions. The C(1)/C(3) ratio derived from monolabeled substrates deviates significantly from unity, the theoretical value expected for complete β-oxidation of butyrate to acetyl-CoA. C(1) labeling of butyrate leads to C(1)/C(3) ratios of about 2; C(3) labeling, to those of 0.3–0.5. This provides qualitative evidence that a considerable fraction of the substrate (about 40–50%) is converted to acetoacetyl-CoA whereas the rest undergoes β-oxidation to acetyl-CoA. Second, for a given substrate the C(1)/C(3) ratios appear to be little influenced by the hormonal state of the animal. This result is rather surprising since the pool of nonlabeled acetyl-CoA is distinctly larger in the diabetic animal. The data can be explained, however, if it is assumed that the direct conversion of butyrate to acetoacetyl-CoA is enhanced in the diabetic animal as compared to the fasted animal. Hence, the dilution of [1-^{13}C]acetyl-CoA by endogenous acetyl-CoA in the diabetic state would be compensated by channeling less ^{13}C-labeled butyrate into the pathway of β-oxidation to acetyl-CoA.

The mechanism of ketone body formation from butyrate has been investigated previously with rat liver slices and isolated mitochondria (Hird & Symons, 1962). Radioactively labeled [1-^{14}C]butyrate and [3-^{14}C]butyrate were tested as substrates, and the results demonstrated a substantial asymmetry in the incorporation of ^{14}C into C(1) as compared to C(3) of the ketone bodies formed. The C(1)/C(3) ratios for [1-^{14}C]-butyrate and [3-^{14}C]butyrate were about 4 and 0.35, respectively. Smaller asymmetries of incorporation with C(1)/C(3) ratios of about 1.5 were observed for long-chain fatty acids (Schumann et al., 1978; Ohgaku et al., 1982). The purpose of these earlier studies was to estimate the contribution of two different pathways for the conversion of acetoacetyl-CoA to acetoacetate, namely either direct deacylation or the more complex (hydroxymethyl)glutaryl-CoA pathway. It is generally agreed now that the latter is the major pathway for the formation of acetoacetate. In contrast, the present studies focus the attention not on the disposal but on the formation of acetoacetyl-CoA. The large asymmetry in the ^{13}C labeling pattern of 3-hydroxybutyrate can only be generated by direct conversion of labeled butyrate to acetoacetyl-CoA but not via β-oxidation to acetyl-CoA.

ACKNOWLEDGMENTS

We thank P. Ganz for the competent synthesis of ^{13}C-labeled butyric acids.

Registry No. Acetyl-CoA, 72-89-9; $PrCO_2H$, 107-92-6; AcAcOH, 541-50-4; $MeCH(OH)CH_2CO_2H$, 300-85-6; HCO_3^-, 71-52-3; L-glutamate, 56-86-0; L-glutamine, 56-85-9; D-glucose, 50-99-7; insulin, 9004-10-8.

REFERENCES
Aas, M., & Bremer, J. (1968) *Biochim. Biophys. Acta 164*, 157–166.
Alger, J. R., Behar, K. L., Rothman, D. L., & Shulman, R. G. (1984) *J. Magn. Reson. 56*, 334–337.
Bates, M. W., Krebs, H. A., & Williamson, D. H. (1968) *Biochem. J. 110*, 655–661.
Berry, M. N., Gregory, R. B., Grivell, R. A., & Wallace, P. G. (1983) *Eur. J. Biochem. 131*, 215–222.
Blackshear, P. J., & Alberti, K. G. M. (1974) *Biochem. J. 138*, 107–117.
Cahill, G. F. (1981) *J. Parent. Ent. Nutr. 5*, 281–287.
Canioni, P., Alger, J. R., & Shulman, R. G. (1983) *Biochemistry 22*, 4974–4980.
Cross, T. A., Pahl, C., Oberhänsli, R., Aue, W. P., Keller, U., & Seelig, J. (1984) *Biochemistry 23*, 6398–6402.
Cross, T. A., Müller, S., & Aue, W. P. (1985) *J. Magn. Reson. 62*, 87–98.
Heussler, A., Ganz, P., & Gäumann, T. (1975) *J. Labelled Compd. 11*, 37–42.
Hird, F. J. R., & Symons, L. P. (1962) *Biochem. J. 84*, 212–216.
Lynen, F., Henning, U., Bublitz, C., Sorbö, B., & Kröplin-Rueff, L. (1958) *Biochem. Z. 330*, 269–295.
Mayes, P. A., & Laker, M. E. (1981) *Biochem. Soc. Trans. 9*, 339–341.
McGarry, J. D., & Foster, D. W. (1971) *J. Biol. Chem. 264*, 1149–1159.
McGarry, J. D., & Foster, D. W. (1980) *Annu. Rev. Biochem. 49*, 395–420.
Ohgaku, S., Brady, P. S., Schumann, W. C., Bartsch, G. E., Margolies, J. M., Kumaran, K., Landau, S. B., & Landau, B. R. (1982) *J. Biol. Chem. 257*, 9283–9289.
Owen, O. E., & Schramm, V. L. (1981) *Biochem. Soc. Trans 9*, 342–344.
Reo, N. V., Siegfried, B. A., & Ackerman, J. J. H. (1984) *J. Biol. Chem. 259*, 13664–13667.
Schumann, W. C., Hemmelgarn, E., & Landau, B. R. (1978) *Arch. Biochem. Biophys. 190*, 345–350.
Siegfried, B. A., Reo, N. V., Ewy, C. S., Shalwitz, R. A., Ackerman, J. J. H., & McDonald, J. M. (1985) *J. Biol. Chem. 260*, 16137–16142.
Siess, E. A., Kientsch-Engel, R. I., & Wieland, O. H. (1982) *Eur. J. Biochem. 121*, 493–499.
Stevens, A. N., Iles, R. A., Morris, P. G., & Griffiths, J. R. (1982) *FEBS Lett. 150*, 489–493.
Stromski, M. E., Arias-Mendoza, F., Alger, J. R., & Shulman, R. G. (1986) *Magn. Res. Med. 3*, 24–32.
Wieland, O. H. (1968) *Adv. Metab. Disord. 3*, 1–47.
Williamson, D. H. (1979) *Biochem. Soc. Trans. 7*, 1313–1320.

Absolute Stereochemistry of Flavins in Enzyme-Catalyzed Reactions†

Dietmar J. Manstein and Emil F. Pai*
Department of Biophysics, Max Planck Institute for Medical Research, D-6900 Heidelberg, Federal Republic of Germany
Lawrence M. Schopfer and Vincent Massey
Department of Biological Chemistry, The University of Michigan, Ann Arbor, Michigan 48109
Received April 28, 1986; Revised Manuscript Received July 10, 1986

ABSTRACT: The 8-demethyl-8-hydroxy-5-deaza-5-carba analogues of FMN and FAD have been synthesized. Several apoproteins of flavoenzymes were successfully reconstituted with these analogues. This and further tests established that these analogues could serve as general probes for flavin stereospecificity in enzyme-catalyzed reactions. The method used by us involved stereoselective introduction of label on one enzyme combined with transfer to and analysis on a second enzyme. Using as a reference glutathione reductase from human erythrocytes for which the absolute stereochemistry of catalysis is known from X-ray studies [Pai, E. F., & Schulz, G. E. (1983) *J. Biol. Chem. 258*, 1752–1758], we were able to determine the absolute stereospecificities of other flavoenzymes. We found that glutathione reductase (NADPH), general acyl-CoA dehydrogenase (acyl-CoA), mercuric reductase (NADPH), thioredoxin reductase (NADPH), *p*-hydroxybenzoate hydroxylase (NADPH), melilotate hydroxylase (NADH), anthranilate hydroxylase (NADPH), and glucose oxidase (glucose) all use the *re* face of the flavin ring when interacting with the substrates given in parentheses.

FAD and FMN are ubiquitous coenzymes. They are extremely versatile redox catalysts, taking part in radical, carbanion, or hydride-transfer mechanisms (Hamilton, 1971; Hemmerich, 1976; Bruice, 1980; Walsh, 1980). They therefore occupy a central position in enzyme-catalyzed redox chemistry. At present, there are far more than 100 different flavoenzymes known, most of them members of the class of oxidoreductases (*Enzyme Nomenclature*, 1984).

Enzymatic (Jorns & Hersh, 1974; Fisher & Walsh, 1974; Hersh & Walsh, 1981; Thorpe & Williams, 1976) as well as bioorganic model studies (Brüstlein & Bruice, 1972; Loechler & Hollocher, 1980) have made it clear that positions C4α and N5 are the key loci of interaction between flavins and substrates. A common mechanism that has been proposed for many flavoenzymes involves the transfer of the equivalent of

† Supported, in part, by Grant GM-1106 from the U.S. Public Health Service. This work has also been submitted by D.J.M. to the University of Heidelberg in partial fulfillment of the requirements for the Ph.D. degree.

0006-2960/86/0425-6807$01.50/0